Journal of Earth Science, *Vol. 35*, *No. 1*, *p. 177–189*, *February 2024* *ISSN 1674-487X*
Printed in China
https://doi.org/10.1007/s12583-021-1522-z

Influence of Sub-Cloud Secondary Evaporation Effects on the Stable Isotopes in Precipitation of Urumqi Glacier No. 1, Eastern Tianshan

Mengyuan Song[1], **Zhongqin Li**[*1, 2, 3], **Feiteng Wang**[1], **Xin Zhang**[1]
1. *State Key Laboratory of Cryospheric Sciences*, *Northwest Institute of Eco-Environment and Resources*, *Tianshan Glaciological Station*, *Chinese Academy of Sciences*, *Lanzhou* 730000, *China*
2. *College of Geography and Environmental Science*, *Northwest Normal University*, *Lanzhou* 730000, *China*
3. *College of Sciences*, *Shihezi University*, *Shihezi* 832000, *China*
Zhongqin Li: https://orcid.org/0000-0002-2667-9977

ABSTRACT: In arid regions, the stable hydrogen and oxygen isotopic composition in raindrops is often modified by sub-cloud secondary evaporation when they descend from cloud base to ground through the unsaturated air. As a result of kinetic fractionation, the slope and intercept of the δ^2H-$\delta^{18}O$ correlation equation decrease. The variation of deuterium excess from cloud base to the ground is often used to quantitatively evaluate the influence of secondary evaporation effect on isotopes in precipitation. Based on the event-based precipitation samples collected at Urumqi Glacier No. 1, eastern Tianshan during four-year observation, the existence and impact of secondary evaporation effects were analyzed by the methods of isotope-evaporation model. Under high air temperature, small raindrop diameter and precipitation amount, and low relative humidity conditions, the remaining rate of raindrops is small and the change of deuterium excess is large relatively, and the slope and intercept of δ^2H-$\delta^{18}O$ correlation equation are much lower than those of Global Meteoric Water Line, which mean that the influence secondary evaporation on precipitation enhanced. While on the conditions of low air temperature, high relative humidity, heavy rainfall, and large raindrop diameter, the change of deuterium excess is small relatively and the remaining rate of raindrops is large, and the slope and intercept of δ^2H-$\delta^{18}O$ correlation equation increase, the secondary evaporation is weakened. The isotope-evaporation model described a good linear correlation between changes of deuterium excess and evaporation proportion with the slope of 0.90‰/%, which indicated that an increase of 1% in evaporation may result in a decrease of deuterium excess about 0.90‰.

KEY WORDS: stable isotopes, meteoric water line, deuterium excess, sub-cloud secondary evaporation effect, precipitation, glaciers.

0 INTRODUCTION

The alpine mountains around the world are the birthplaces of many rivers, while the ecological environment and hydrometeorological factors in the region are very fragile. The runoff process and the change of components in the basin are very sensitive to climate change, which affects the runoff and water resources quality of the whole flow region from upstream to downstream. In the high-latitude and polar alpine mountain region, the main supply source of river is meltwater from glaciers and snow cover. Different from the high-latitude basin. The contribution of precipitation recharge to the rivers in the middle and low latitude Alpine Basin cannot be ignored. Based on the above research background, further research on precipitation will help us better understand the water cycle of inland river basins in alpine and cold regions (Yu et al., 2010). The stable hydrogen and oxygen isotopic composition in precipitation is primarily affected by evaporation and condensation and is an ideal tracer for studying water cycle and climate system changes through the isotope Rayleigh fractionation model (Cao et al., 2021; Wang and Liu, 2020; Li et al., 2019; Wang X Y et al., 2015; Peng et al., 2007; Pande et al., 2000). For raindrops falling from the cloud base to the ground, due to the influence of evaporation, the isotopic values will vary (Christner et al., 2018; Li et al., 2018; Kong et al., 2016; Wang et al., 2016). The evaporation effect experienced by raindrops from the cloud base to the ground is called sub-cloud secondary evaporation. During the evaporation of raindrops in the unsaturated air, affected by non-equilibrium fractionation and kinetic fractionation, the heavy isotopes are enriched and the deuterium excess decreased in the raindrops (Liu et al., 2008; Jouzel and Merlivat, 1984; Yapp, 1982; Stewart, 1975; Dansgaard, 1964).

*Corresponding author: lizq@lzb.ac.cn

Manuscript received March 13, 2021.
Manuscript accepted July 26, 2021.

Song Mengyuan, Li Zhongqin, Wang Feiteng, Zhang Xin, 2024. Influence of Sub-Cloud Secondary Evaporation Effects on the Stable Isotopes in Precipitation of Urumqi Glacier No. 1, Eastern Tianshan. *Journal of Earth Science*, 35(1): 177–189. https://doi.org/10.1007/s12583-021-1522-z. http://en.earth-science.net

During using isotope methods to analyze the water cycle process, qualitative descriptions can no content the demand of parameterization stimulation method. It is necessary to quantify the influence of sub-cloud secondary evaporation on isotopes in precipitation. The deuterium excess (abbreviated as *d*-excess hereafter, defined as $d = \delta^2H - 8\delta^{18}O$), as the second-order isotopic parameter of stable oxygen and hydrogen isotopes, is mainly affected by the relative humidity, sea temperature, and other meteorological conditions in the water vapor source area, which can be used as an essential parameter to trace the water vapor source (Jouzel and Merlivat, 1984; Merlivat and Jouzel, 1979). Besides, the slopes of δ^2H-$\delta^{18}O$ correlation in precipitation will also decrease, which possibly by the kinetic isotope effect in the sub-cloud secondary evaporation (Stewart, 1975; Dansgaard, 1964). Previous researches have used the variation of $\delta^{18}O$, δ^2H, slope of δ^2H-$\delta^{18}O$ correlation, and *d*-excess values in precipitation to assess the sub-cloud secondary evaporation effect and influencing factors, and also made the quantitative assessment. Based on the experimental observations, Stewart (1975) researched the stable isotope change in raindrops during the evaporation in different gas environments, who also established a model of the falling water drops. The model and its improvement scheme had a significant influence on subsequent studies of sub-cloud secondary evaporation and isotope fractionation. In recent years, based on various improved Stewart models, a large number of quantitative studies have been made on the sub-cloud secondary evaporation in different regions, which has enriched the understanding of the seasonal patterns and regional differences of the sub-cloud secondary evaporation in typical areas (Li et al., 2016b; Ma et al., 2014). However, subsequent studies found that this back-calculation algorithm may contain a large amount of uncertainty.

Northwestern China located in the hinterland of Eurasia is far from the sea. The water vapor from the ocean can rarely reach the region, mainly from Europe and central Asia, which makes drought a major climatic characteristic of the area (Song et al., 2019; Wang et al., 2017). In arid environment, raindrops are more susceptible to evaporation when they pass through the unsaturated atmosphere (Salamalikis et al., 2016; Wang et al., 2016; Peng et al., 2007). Northwest China has the conditions for the occurrence of secondary evaporation under the clouds. Therefore, many researchers not only used stable isotope tracer to analyze the difference in the spatial and temporal distribution of different water bodies (such as precipitation and meltwater) but also investigated the effect of sub-cloud evaporation in precipitation in Northwest China (Chen H Y et al., 2020; Ma et al., 2020; Li et al., 2016a; Zhu et al., 2016; Chen F L et al., 2015). In the Urumqi River Basin, some scholars analyzed the *d*-excess value in precipitation to determine the change in isotopic composition of precipitation affected by secondary evaporation sub-cloud (Kong and Pang, 2016; Kong et al., 2013; Pang et al., 2011). Feng et al. (2013) compared the differences of isotopes in precipitation and evaporation in the headwaters of low altitude mountains and high altitude rivers in Urumqi River Basin. By simulating the temperature effect of stable isotope, Zhang et al. (2003) found that precipitation attenuated isotopic composition to a great extent after long-distance transportation. Liu J R et al. (2014) used the Chinese Network of Isotopes in Precipitation (CHNIP) data to investigate the precipitation isotopes, and found the highly consistent between Fukang and Urumqi. According to the parameter optimization of Stewart model, the secondary evaporation intensity of more than 20 stations around the Tianshan was studied, and the results showed that the isotopic composition changed in different degrees during the raindrop from the cloud to the ground at different locations (Wang et al., 2016). At Urumqi Glacier No. 1, the relationship between meteorological parameters and isotopic composition of precipitation, meltwater, and river water was researched, and that the moisture at Urumqi Glacier No. 1 mostly come from the local source (Song et al., 2019). According to the water samples collected in Qilian Mountain and Hexi Corridor in China, the researchers made a comprehensive investigation of the water cycle in the basin (Ma et al., 2020; Li et al., 2019). In recent years, the researches of evaporation mechanism in precipitation in Northwest China have also emerged gradually. The researchers mainly concentrated on the stable isotopic composition changes in precipitation. However, the systematic investigation on the variation of isotopc composition in raindrops falling from cloud base to ground, and the internal mechanism of the sub-cloud secondary evaporation and isotopic composition in precipitation at the glacierized area is still unclear, which need further discussion. In the case of generally rising temperature (Zheng et al., 2019) and the changing trend of accelerated glacier melting(Wang P Y et al., 2015, 2014; Li et al., 2011), it is necessary to assess the effect of sub-cloud evaporation on raindrops in Urumqi Glacier No. 1. Therefore, based on the four-year monitoring of event-based precipitation samples at Urumqi Glacier No. 1, the purpose of this study was to the influence of sub-cloud secondary evaporation on precipitation at the glacierized area by using the methods of isotope evaporation model and the ordinary least squares (OLSR) regression.

1 MATERIALS AND METHODS

1.1 Data and Site Description

Northwest China lies in the hinterland of Eurasia in the mid-latitude zone, is the innermost center of the Eurasia continent. The long-distance from the ocean will lead to a dry climate in the area, which is sensitive to global climate change (Shi et al., 2007). Tianshan is the most extensive zonal mountain system in Central Asia, and the precipitation is relatively abundant due to the blocking effect of high mountains on water vapor. Tianshan has a large number of glaciers in Northwest China. The Urumqi River Basin is located in the middle part of the north slope of East Tianshan Mountain (43°00′N–44°07′N, 86°45′E–87°56′E), with an average altitude of 3 083 m (Fig. 1). The headwaters of Urumqi River Basin are mainly composed of exposed rocks and rubble mounds, and the rest are covered by glaciers and snow. There are 7 modern glaciers with a total area of 5.7 km^2 over 3 600 m above sea level in the basin. The altitude of snow line is between 3 800 and 4 200 m. The modern process of glacier erosion and accumulation and periglacial process is very significant. Urumqi Glacier No. 1 (43° 08′N, 86° 82′E) located the headwaters of Urumqi River Basin is the best-monitored glacier with the most extended da-

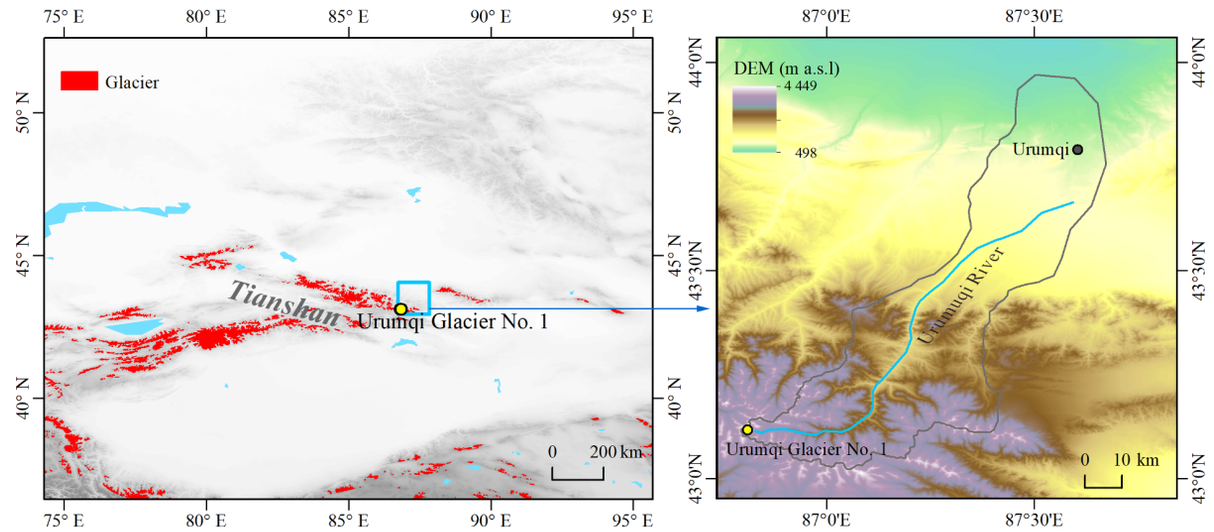

Figure 1. Map showing the location and sampling sites. The polygons filled with red represent glaciers.

ta series (Fig. 1). Urumqi Glacier No. 1 is a northwest-facing valley glacier, with an altitude of 3 743 to 4 484 m a.s.l. It melted rapidly and separated into two branches in 1993, consisting of the east branch (1.086 km^2) and west branch (0.591 km^2) (Xu et al., 2019). The Urumqi Glacier No. 1 has a trend of accelerated shrinking, with the decrease in area and thickness, and the retreat at the terminus of the glacier (Ding et al., 2019).

According to the observation data of Daxigou meteorological station which is located 3 km downstream of Urumqi Glacier No. 1 (Feng et al., 2013). During the four-year observation period from January 2008 to December 2011, the annual average temperature in the headwaters of Urumqi River Basin is about -4.1 ℃, ranging from -16.1 ℃ in January to 5.6 ℃ in August, and the temperature is above 0 ℃ in May to September, and the annual mean precipitation amount is about 700 mm (Song et al., 2019). The precipitation mainly occurs in summer, but less in winter, and even no precipitation in some months.

There were 206 event-based precipitation samples collected from May to October 2008 to 2011 at Urumqi Glacier No. 1 (Fig. 1), and each of which was obtained strictly according to the requirements of the meteorological observation standard (Liu B et al., 2014). At the beginning of each precipitation event, we opened two collection containers installed at a height of 1 m above the ground. After the rainfall event, we cleaned the high-density polyethylene bottles with rainwater from one container and then collected the rainwater from another one immediately to minimize evaporation or diffusion. The solid samples include snow and hail were sealed in zip-lock LDPE bags and melted at room temperature before being filled into the high-density polyethylene bottles. We also recorded the concurrent meteorological parameters at the beginning and end of each event, such as temperature, precipitation amount, and relative humidity. All the samples were transported and stored frozen at -15 °C until being analyzed at the State Key Laboratory of Cryospheric Sciences, Northwest Institute of Eco-Environment and Resources, Chinese Academy of Sciences (CAS), Lanzhou, China. We used the LWIA DLT-100 (Los Gatos Research) liquid water isotope analyzer to examine the precipitation stable hydrogen and oxygen isotopes, and the sample was gasified at 100 ℃ for determination. Five samples and two isotopic standards were tested as a group, and each sample or isotopic standard was injected six times. The first three injections were discarded due to the memory effect from the residue of the previous sample, and the results of the last three injections were used (Lis et al., 2008). The δ^2H and δ^{18}O values were expressed in ‰ units relative to the V-SMOW (Vienna Standard Mean Ocean Water) are expressed as δ values.

$$\delta^{18}O = \frac{\left(^{18}O/^{16}O\right)_{sample} - \left(^{18}O/^{16}O\right)_{SMOW}}{\left(^{18}O/^{16}O\right)_{SMOW}} \times 10^3‰$$

$$\delta^{18}O = \frac{\left(^{2}H/^{1}H\right)_{sample} - \left(^{2}H/^{1}H\right)_{SMOW}}{\left(^{2}H/^{1}H\right)_{SMOW}} \times 10^3‰$$

The measurement accuracy is ±0.2‰ for δ^{18}O and ±0.6‰ for δ^2H, respectively. The monthly data of samples about δ^2H, δ^{18}O, and *d*-excess are shown in Table 1. The meteorological data of each precipitation are supplied by Daxigou Meteorological Station. Song et al. (2019) described more details of sampling and laboratory analysis.

1.2 Method

Generally, precipitation will show enrichment of stable oxygen and hydrogen isotopes and decrease of *d*-excess influenced by the sub-cloud secondary evaporation, and the slope and intercept of δ^2H-δ^{18}O correlation equation will also change accordingly (Wu et al., 2015). However, this qualitative description cannot meet the current needs of various numerical simulation parameterization. When analyzing the water cycle by isotope method, it is also necessary to make clear what changes occur in the water isotope during the sub-cloud secondary evaporation. In this work, we use two methods to analyze the phenomenon that isotopic modification in the falling raindrops affected by sub-cloud secondary evaporation: Isotope-evaporation model and OLSR regression.

Table 1 The monthly-event weighted values of δ^2H, $\delta^{18}O$ and *d*-excess at ground and cloud base for each year at Urumqi Glacier No. 1 from May to October

Sampling date		δ^2H (‰)	$\delta^{18}O$ (‰)	*d*-excess (‰)			*n*
				Ground	Cloud base	Δd	
2008	May	-40.1	-7.0	15.6	38.7	-23.1	10
	June	-41.7	-6.1	7.4	31.2	-23.8	18
	July	-33.8	-6.0	13.9	24	-10.1	17
	August	-50.1	-8.9	21.1	37.3	-16.2	11
	September	-48.6	-9.4	26.8	38.6	-11.8	10
	October	-111.9	-16.5	20.5	20.5	0.0	3
2009	May	-64.8	-11.4	26.1	26.1	0.0	9
	June	-59.3	-9.4	15.9	22.8	-6.9	13
	July	-39.7	-7.0	16.4	24.7	-8.3	14
	August	-29.8	-4.9	9.4	21.4	-12.0	9
	September	-91.0	-13.7	18.3	27.7	-9.4	8
	October	-78.1	-12.7	23.1	23.1	0.0	4
2010	May	-69.8	-8.3	-3.4	0	-3.4	10
	June	-64.2	-8.6	4.7	12	-7.3	12
	July	-21.5	-3.8	8.7	21.7	-13.0	11
	August	—	—	—	—	—	0
	September	-61.9	-9.4	13.3	14.9	-1.6	3
	October	-114.7	-15.4	8.5	8.5	0	1
2011	May	-61.0	-8.9	10.5	15.7	-5.2	4
	June	-61.3	-9.3	13.5	17.5	-4.0	13
	July	-33.7	-6.7	19.8	31	-11.2	10
	August	-28.6	-5.3	14.0	26.8	-12.8	14
	September	-0.25	-2.3	18.5	33.5	-15.0	2
	October	—	—	—	—	—	0

1.2.1 OLSR regression

The variation of isotopes in precipitation is a physical process of evaporation and condensation, which is related to the meteorological parameters such as air temperature, precipitation amount, atmospheric vapor pressure, and relative humidity (Zhu et al., 2016; Li et al., 2016a; Chen et al., 2015; Peng et al., 2007). The effect of sub-cloud secondary evaporation on isotopes in precipitation makes the values of $\delta^{18}O$ increase and *d*-excess decrease and affects the slope and intercept of the δ^2H-$\delta^{18}O$ correlation equation, $\delta^2H = a\delta^{18}O + b$. By comparing the slope and intercept in the different ranges of meteorological conditions, the secondary evaporation effect can adequately discuss. Therefore, according to the slope and intercept of the δ^2H-$\delta^{18}O$ correlation equation and its deviation from the Global Meteoric Water Line (GMWL), we can understand that the precipitation events are affected by different meteorological parameters and the sub-cloud secondary evaporation (Salamalikis et al., 2016). The slope (*a*) and intercept (*b*) and their standard deviation (σ_a and σ_b) were calculated by ordinary least squares regression (Crawford et al., 2014).

1.2.2 Isotope-evaporation model

Influenced by the sub-cloud secondary evaporation, the stable isotopes of raindrops in the cloud base are different from those in raindrops falling to the ground. According to Froehlich et al. (2008) and Stewart (1975), assuming that cloud base precipitation and the surrounding water vapor reach an isotopic equilibrium state, the change of *d*-excess between the surface precipitation and the cloud base precipitation can be expressed as follow.

$$\Delta d = d - d_{cb} = {}^2F - 8\,{}^{18}F$$

where d and d_{cb} are the *d*-excess value of precipitation at the sampling point and the cloud base, respectively. ${}^2F$ and ${}^{18}F$ are the parameters of ^2H and ^{18}O, and the calculation formulas are as follows.

$${}^2F = \left(1 - \frac{{}^2\gamma}{{}^2\alpha}\right)\left(f^{\,{}^2\beta} - 1\right)$$

$${}^{18}F = \left(1 - \frac{{}^{18}\gamma}{{}^{18}\alpha}\right)\left(f^{\,{}^{18}\beta} - 1\right)$$

where f is the residual fraction of the mass of raindrop after evaporation, ${}^2\alpha$ and ${}^{18}\alpha$ are the equilibrium fractionation coefficients of ^2H and ^{18}O, respectively (Criss, 1999).

$${}^2\alpha = \exp\left(\frac{24.844 \times 10^3}{T^2} - \frac{76.248}{T} + 52.612 \times 10^{-3}\right)$$

$${}^{18}\alpha = \exp\left(\frac{1.137 \times 10^3}{T^2} - \frac{0.415\,6}{T} - 2.066\,7 \times 10^{-3}\right)$$

where T is the air temperature at lifting condensation level in K, the parameters γ and β were calculated as follows.

$${}^2\gamma = \frac{{}^2\alpha RH}{1 - {}^2\alpha\left({}^2D/{}^2D'\right)^n(1 - RH)}$$

$${}^{18}\gamma = \frac{{}^{18}\alpha RH}{1 - {}^{18}\alpha\left({}^{18}D/{}^{18}D'\right)^n(1 - RH)}$$

$${}^2\beta = \frac{1 - {}^2\alpha\left({}^2D/{}^2D'\right)^n(1 - RH)}{{}^2\alpha\left({}^2D/{}^2D'\right)^n(1 - RH)}$$

$${}^{18}\beta = \frac{1 - {}^{18}\alpha\left({}^{18}D/{}^{18}D'\right)^n(1 - RH)}{{}^{18}\alpha\left({}^{18}D/{}^{18}D'\right)^n(1 - RH)}$$

where RH is relative humidity in decimal; n is 0.58; D and D' are diffusion coefficients of water and heavy water in the atmosphere. The values of ${}^2D/{}^2D'$ and ${}^{18}D/{}^{18}D'$ are 1.024 and 1.028 9, respectively (Stewart, 1975).

In the model of Froehlich et al. (2008), it was not clear how to calculate the residual fraction of raindrop evaporation. In this study, we used a method by Wang et al. (2016) to consider the remaining rate of raindrops as the mass change of water droplets from the cloud base to the ground surface.

$$f = \frac{m_{end}}{m_{end} + m_{ev}}$$

where m_{end} is the mass of raindrops reaching the ground, and m_{ev} is the mass lost by evaporation which can define as

$$m_{ev} = E_{ev}t$$

where E_{ev} and t represent the evaporation intensity and fall time of raindrop, respectively. The falling time is

$$t = \frac{H_{cb}}{v_{end}}$$

where H_{cb} is the height of the cloud base in m and v_{end} is the final velocity of a raindrop in m/s. The shape change of raindrops is ignored and regarded as spherical, and its mass can express as

$$m_{end} = \frac{4}{3}\pi r_{end}^3 \rho$$

where r_{end} is the radius of the raindrops, and ρ is the density of water.

Raindrop evaporation rate can be calculated following (Kinzer and Gunn, 1951).

$$E_{ev} = Q_1 Q_2$$

Q_1 is a function of ambient temperature and diameter of a raindrop in cm; Q_2 is a function of ambient temperature and relative humidity in g/(cm·s). In this study, we use the experimental data of Kinzer and Gunn (1951) and use bilinear interpolation to obtain Q_1 and Q_2 under different meteorological conditions (Wang et al., 2016).

The following formula calculates the end velocity of a raindrop.

$$v_{end} = \begin{cases} 9.58e^{0.035\,4H_{cb}}\left[1 - e^{-\left(\frac{D}{1.77}\right)^{1.147}}\right], 0.3 \leqslant D < 6.0 \\ 1.88e^{0.025\,6H_{cb}}\left[1 - e^{-\left(\frac{D}{1.304}\right)^{1.817}}\right], 0.05 \leqslant D < 0.3 \\ 28.40D^2 e^{0.017\,2H_{cb}}, D < 0.05 \end{cases}$$

Here, D is diameter of raindrops in mm. H_{cb} calculates by lifting condensation level (Fletcher and Bretherton, 2010).

$$H_{cb} = 18\,400\left(1 + \frac{t_{\text{mean}}}{273}\right)\lg\frac{P_0}{P_{LCL}}$$

t_{mean} is the average temperature (℃) between lifting condensation level and surfaces, which calculates by the arithmetic mean value of the air temperature between the surface and LCL; P_0 and P_{LCL} are air pressure (hPa) at surface and LCL.

$$P_{LCL} = P_0\left(\frac{T_{LCL}}{T_0}\right)^{3.5}$$

T_{LCL} and T_0 are air temperature (K) at LCL and surface. T_{LCL} calculates by the empirical formula (Barnes, 1968).

$$T_{LCL} = T_d - \left(0.001\,296T_d + 0.196\,3\right)\left(T_0 - T_d\right)$$

where T_d and T_0 are the dew point temperature and surface air temperature (℃) at the sampling site. According to an assessment of multiple empirical formulas by Górnicki et al. (2017), the optimal equation in determining the dew point is

$$T_d = \frac{237\left(\lg RH + \frac{7.5T}{237 + T}\right)}{7.5 - \lg RH - \frac{7.5T}{237 + T}}$$

where T_d and T are dew point and air temperature in °C, and RH is relative humidity in decimal.

The raindrops diameter can be calculated by an empirically derived formula as follow (Wang et al., 2021).

$$D = 0.474\,8 + 1.459\,6\left(1 - e^{-0.124\,3P}\right)$$

where P is daily precipitation amount in mm.

2 RESULTS AND DISCUEEION

2.1 Variations of *d*-Excess in Precipitation and Water Lines for Different Meteorological Conditions

2.1.1 Influence of precipitation amount

According to 206 event-based precipitation samples collected at Urumqi Glacier No. 1 from May 2008 to October 2011, the δ^2H-δ^{18}O correlation equation of the initial value of isotopes in precipitation obtained, and the correlation equation of δ^2H-δ^{18}O can be calculated as follow.

$$\delta^2\text{H} = 7.08\delta^{18}\text{O} + 6.18, R^2 = 0.93$$

We weighted the monthly precipitation of hydrogen and oxygen isotopes in the collected precipitation samples, and obtained the linear correlation equation of δ^2H and δ^{18}O based on the amount-weighted monthly average of precipitation.

$$\delta^2\text{H} = 7.46\delta^{18}\text{O} + 11.33, R^2 = 0.93$$

The slope of the δ^2H-δ^{18}O correlation equation at Urumqi Glacier No. 1 is lower than that of GMWL, both on event-based and monthly-weighted. However, the slope in initial precipitation is different from that in the monthly precipitation. As a result, the difference in the slope of meteoric water lines between event-based precipitation samples and monthly-weighted precipitation samples may be related to the isotopic composition of minor rainfall events (Peng et al., 2010). To further explain the reason for the difference and analyze the influence of sub-cloud secondary evaporation, all the 206 precipitation samples were classified into rainfall and snowfall. Rainfall events were further divided into five groups with different gradient ranges according to the precipitation amount (Table 2). In this study, the slope of the δ^2H-δ^{18}O correlation equation in 18 snow samples is 8.68, which is above the slope (8) of GMWL and indicates that the influence of the secondary evaporation on snowfall is weak. Moreover, the slope (7.08) and the intercept (6.18) of all the initial precipitation samples are higher than that in all the rainfall samples, mainly due to the impact of snowfall events. The rain is more susceptible to secondary evaporation than snowfall during precipitation.

As shown in Table 2, with the decreasing of rainfall amount, the values of *d*-excess, slope and intercept of the δ^2H-δ^{18}O correlation equation have also decreased. The *d*-excess in raindrops decreased from 18.58‰ (P > 15 mm) to 8.39‰ (0 mm < P ⩽ 1 mm). The slope decreased from 7.04 (P > 15 mm) to 6.51 (0 mm < P ⩽ 1 mm), while the intercept decreased from 10.36‰ (P > 15 mm) to 0.31‰ (0 mm<P ⩽ 1 mm). The reason for these differences of slope should be that in small rainfall events, the water vapor pressure is an unsaturated state in which the raindrops evaporate with isotope fractionation (Dansgaard, 1964). While in the larger rainfall events, the atmospheric moisture content is close to saturated, and the secondary evaporation is weak (Wang et al., 2016; Zhu et al., 2016). The slope and intercept of δ^2H-δ^{18}O correlation equation in precipitation are reduced due to the isotope fractionation by the influ-

Table 2 Number of samples, total precipitation amounts, and δ^2H-$\delta^{18}O$ correlation parameters for snow and rain (different amount ranges) collected at Urumqi Glacier No. 1

Samples	Number of samples	*d*-excess (‰)	Slope	Intercept (‰)	R^2
Total Samples	206	12.69	7.08 ± 0.14	6.18 ± 1.27	0.93
Snow Samples	18	16.30	8.68 ± 0.38	23.43 ± 4.33	0.97
Rain Samples	188	12.04	6.96 ± 0.14	5.31 ± 1.30	0.93
0–1 mm	20	8.39	6.51 ± 0.46	0.31 ± 3.56	0.92
1–2 mm	19	8.24	6.29 ± 0.44	-0.46 ± 3.23	0.92
2–5 mm	57	10.80	7.43 ± 0.24	6.93 ± 2.14	0.95
5–15 mm	78	15.20	7.0 ± 0.23	7.15 ± 2.17	0.93
> 15 mm	14	18.58	7.04 ± 0.96	10.36 ± 8.81	0.82

ence of secondary evaporation and isotopic exchange in raindrops during landing (Stewart, 1975). The stronger the kinetic fractionation, especially the raindrops in small precipitation events, the lower the slope, and intercept of the δ^2H-$\delta^{18}O$ correlation equation, the secondary evaporation is more intense (Zhu et al., 2016; Chen et al., 2015).

2.1.2 Influence of air temperature

The 188 rainfall samples are divided into three groups according to different air temperature ranges, and the fitting parameters of δ^2H-$\delta^{18}O$ correlation equation are analyzed within each interval. The values of $\delta^{18}O$ and *d*-excess, slope, and intercept of δ^2H-$\delta^{18}O$ correlation equation in individual precipitation events collected at different temperature intervals are shown in Table 3. Among all the rain samples, when temperature increased from the range of $T \leqslant 0$ ℃ to the range of $T \geqslant 5$ ℃ in the three intervals, the values of *d*-excess and the slope decreased from 15.5‰ to 8.0‰, and from 7.34 to 6.26, respectively, which indicated that the sub-cloud secondary evaporation effect was more intense with the increasing of temperature. While the values of $\delta^{18}O$ increased from -12.4‰ to -3.1‰ with the increasing of temperature, which showed a visible temperature effect of precipitation isotope at Urumqi Glacier No. 1 (Song et al., 2019; Dansgaard, 1964). The variation of isotopes in precipitation was related to the temperature around the water vapor when it condensed. When the hot air rises to the low-pressure region, adiabatic expansion and thermal radiation lead to the cooling of air mass (Fontes, 1980). Compared with the low temperature, the sub-cloud secondary evaporation is more intense at the high temperature, and the effect of secondary evaporation is more evident than that at the low temperature. When air temperature reaches dew point temperature, atmospheric water vapor condenses in thermodynamic equilibrium to form precipitation. As the air mass carrying water vapor moves from its water vapor source to the continent, it may continually experience condensation and precipitation processes, leaving the air mass with less water vapor. Along with the path of air mass, the δ^2H and $\delta^{18}O$ are continuously distilled from the water vapor during precipitation. With the transformation of water from solid to liquid and gaseous states, heavy isotopes are distilled with the vapor during evaporation fractionation. Based on the Rayleigh distillation, the isotopes δ^2H and $\delta^{18}O$ in the water vapor gradually decrease. The correlation equation of δ^2H-$\delta^{18}O$ is influenced by temperature and isotopic values.

2.1.3 Influence of relative humidity

The rainfall and snowfall are affected by secondary evaporation differently from cloud base to ground, especially for small rainfall (Wang et al., 2016; Zhu et al., 2016; Chen et al., 2015). Therefore, the rainfall samples are further divided into light rainfall (0 mm < $P \leqslant 5$ mm, $n = 96$) and snow samples ($n = 18$). The light rainfall and snow samples were grouped according to different ranges of relative humidity to investigate the effect of relative humidity on the slope of δ^2H-$\delta^{18}O$ correlation equation (Fig. 2).

The slope and intercept of the rainfall samples (0 mm < P < 5 mm) vary greatly, with the average values being 7.25‰ and 6.01‰ respectively, and the maximum variations being 26.25% and 468.33% respectively. The slope and intercept of the snow samples vary slightly, with the average values being 8.53‰ and 22.38‰, respectively, and the maximum changes being 5.05% and 7.18%, respectively. The slope of light rainfall samples changes obviously than that of snow samples. When the relative humidity and the rainfall were large, the variation of slope was slightly. The influence by the relative humidity on the slope is greatly in light rainfall samples. The *d*-excess value in light rainfall samples (0 mm < P < 5 mm) has a large change with the average value of 12.6‰, and the maximum variation is 131.24%. The variation of *d*-excess value in snow samples is tiny, and the average value is 16.7‰, and the maximum variation amplitude is 53.99%.

Due to the isotope fractionation of non-equilibrium secondary evaporation, rainwater is enriched in heavy isotopes and has higher hydrogen and oxygen heavy isotope values. Un-

Table 3 Observed data parameter values which isotopic characteristics affected by the temperature at Urumqi Glacier No. 1

Temperature (℃)	Number of samples	*d*-excess (‰)	Slope	Intercept (‰)	R^2
≤0	35	15.5	7.34 ± 0.53	7.24 ± 6.98	0.85
0–5	100	14.2	7.04 ± 0.22	7.04 ± 1.92	0.91
≥5	53	8.0	6.26 ± 0.27	2.52 ± 1.57	0.90

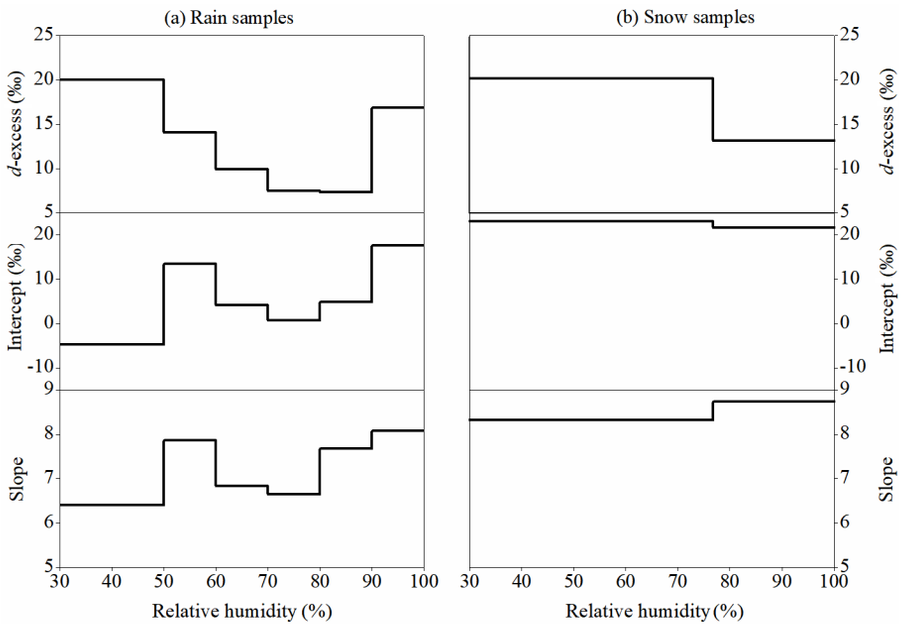

Figure 2. The effect of secondary evaporation influenced by relative humidity for small rain samples ((a), 0 mm < $P \leqslant 5$ mm) and snow samples (b).

der conditions of gradually increasing rainfall or continuous rainfall, the water vapour content of the atmosphere gradually becomes saturated, and the relative humidity gradually increases. The secondary evaporation is weaker, leading to depletion of heavy isotopes in the raindrops. As the relative humidity decreases, the secondary evaporation is significantly enhanced, *d*-excess values decrease, and the $\delta^{18}O$ increased in precipitation influenced by the sub-cloud secondary evaporation. Conversely, when the relative humidity increases, the secondary evaporation relatively weaken. Precipitation is mostly concentrated in the spring and summer seasons, and the lower *d*-excess in precipitation events is influenced by secondary evaporation of stable isotopes during precipitation, especially for some precipitation processes with small amounts and shorter duration (Meng and Liu, 2010). Therefore, we consider that the effect on precipitation by relative humidity likely reflects the secondary evaporation at Urumqi Glacier No. 1.

2.2 Variations of Raindrop Evaporation and Δ*d*

The evaporation intensity of raindrops (E_{ev}) at Urumqi Glacier No. 1 ranges from 0.05 to 2.37 μg·s^{-1}, with an average value of 0.67 μg·s^{-1} and a median value of 0.60 μg·s^{-1}. Because of the high temperature and high evaporation intensity, the evaporation rate of raindrops increased from July to September, and the increase was comparable in the four-year observation period (Fig. 3). Previous researches had also shown that the evaporation intensity of raindrops presented a seasonal variation of high in summer and low in winter, mainly due to the vigorous evaporation by high temperatures in summer. In contrast, the evaporation was weaker in winter when the air temperature was usually below zero (Wang et al., 2016, 2013). In this study, the temperature of the snowfall events was all less than 0 ℃, the drop evaporation was negligible and the residual fractions were close to 100%. Therefore, we only need to calculate the variation of *d*-excess in raindrops falling from the base of clouds to the ground during rainfall events in this study.

The residual fraction of raindrop mass after evaporation (*f*) is one of the essential parameters of secondary evaporation. The value of *f* in rainfall events at Urumqi Glacier No. 1 is calculated by formulas 7 to 17. Based on the droplet experiment

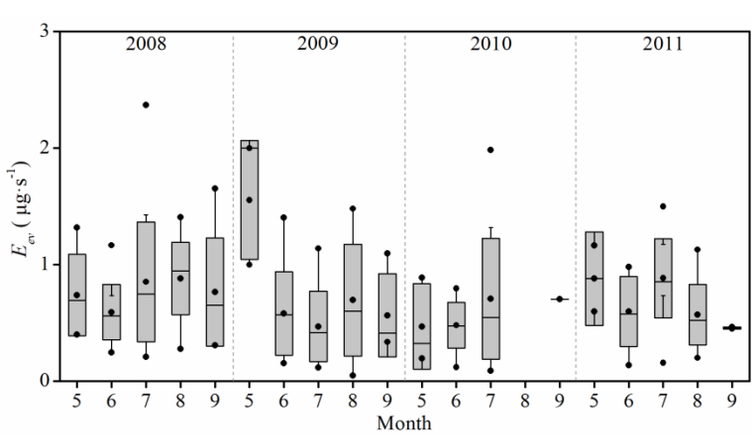

Figure 3. Monthly variation of E_{ev} in precipitation at Urumqi Glacier No. 1.

and the effect of sub-cloud secondary evaporation, these formulas are generally used in liquid precipitation and liquid-solid mixed precipitation (Froehlich et al., 2008). Besides, combined with the meteorological conditions during the precipitation events, we can judge whether there is sub-cloud secondary evaporation effect in the mixed precipitation samples. Therefore, we only calculated the residual fraction of raindrop mass after evaporation at Urumqi Glacier No. 1, but not the snow samples or other solid precipitation. The *f* values in raindrops at Urumqi Glacier No. 1 range from 27.07% to 100%. As shown in Fig. 4, the *f* values in June to September were relatively higher than that in May, which was primarily due to the higher relative humidity and temperature than that in May. From June to August, the monthly change of *f* was not obvious as the relative humidity variation was not evident, and the *f* began to decline gradually in October. In Tianshan, Wang et al. (2016) have also reported that the variation of *f* values ranged from 6.55% to 99.9%, and the remaining fraction in summer months (from April to October) than that in winter months (from November to March). In our study, the results showed that the residual fraction of raindrop mass was also higher in summer months in the glacierized region with low temperature. Our study is similar to those of the above research, indicating that the residual fraction of raindrop mass at Urumqi Glacier No. 1 represents the essential characteristics of the glacierized area in the arid and semi-arid climate region of alpine basin.

Figure 5 and Table 1 illustrate the monthly variation of *d*-excess values (Δd) in raindrops from the cloud base to surface ground during the four-year observation period at Urumqi Glacier No. 1. The variation of *d*-excess values in daily precipitation varied from -71.4‰ to -0.01‰, and the mean value is -13.5‰. On the monthly basis, the Δd values vary from -23.43‰ to 0, and the mean value is -8.9‰. The Δd values in May were lower than those in June to September, which was primarily due to the lower relative humidity and temperature than that in June to September. From June to August, the monthly change of *f* was not obvious as the relative humidity variation was not evident. The variation of Δd in precipitation is consistent with the residual fraction of raindrop mass (Fig. 4), indicating a correlation between Δd and *f* in precipitation.

2.3 Correlation between *f* and Δd

As demonstrated in Froehlich et al. (2008), the residual fraction of raindrop mass in European Alps was greater than 90%, in which had a linear relationship between *f* and Δd with the slope of the correlation equation of Δd-*f* was close to 1.1‰/%. There is a significant positive correlation (approximately 0.90‰/%) between *f* and Δd of raindrop (Fig. 6), which means that for every 1% increase in *f*, the values of *d*-excess decreases by 0.90‰ at Urumqi Glacier No. 1. When the *f* was higher than 95%, linear relationship between *f* and Δd is good with a slope of 1.04 ($R^2 = 1$), which is closer to 1.1. According to the relationship between *f* and Δd in precipitation at Urumqi

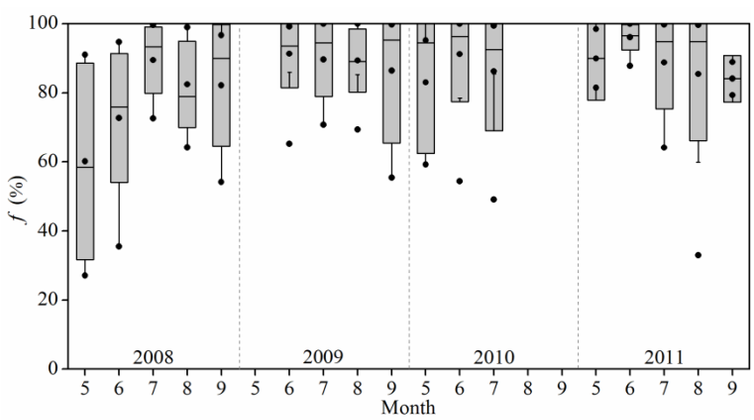

Figure 4. Monthly variation of *f* in precipitation at Urumqi Glacier No. 1.

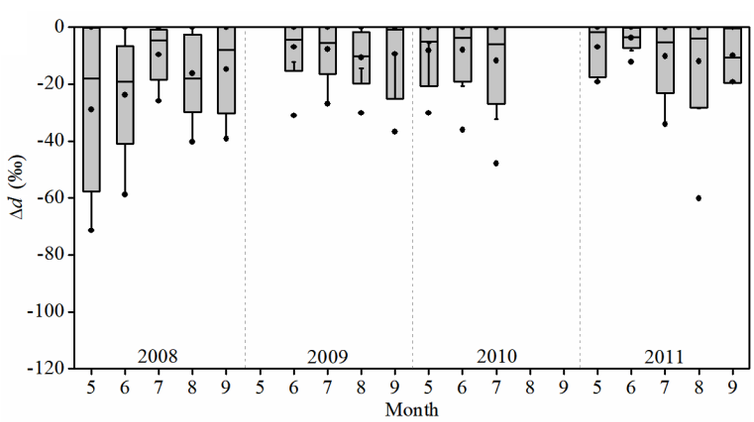

Figure 5. Monthly variation of Δd in precipitation at Urumqi Glacier No. 1.

Glacier No. 1, the slope of linear relationship between *f* and Δ*d* is from 0.85 (2010) to 0.93 (2008) (Table 4). Based on previous studies, when the *f* is above 95%, the correlation between *f* and Δ*d* is approximately 1‰/% (1.1‰/% – 1.2‰/%), which means that for every 1% increase in evaporation, reduction in *d*-excess by approximately 1.1‰ to 1.2‰ (Wang et al., 2016; Kong et al., 2013; Froehlich et al., 2008). With the decrease of evaporation residual ratio, the increase of temperature, and the decrease of relative humidity, the above linear relationship of 1.1‰/% gradually weakens. The linear relationship between the residual fraction of raindrop mass after evaporation and the variation of *d*-excess is 0.9‰/% at Urumqi Glacier No. 1, which indicated that the constant linear relationship of approximately 1.1‰/% was not suitable for Urumqi Glacier No. 1. In our study, many of the mass (The *f* above 95% accounts for 50%) haven't been evaporated when raindrops falling, and the linear relationship between *f* and Δ*d* was apparent. The conclusions obtained under wet conditions in previous studies can also confirm at Urumqi Glacier No. 1. Nevertheless, with decreasing the value of *f*, it is unreasonable to apply the linear relationship of about 1.1‰/% (Wang et al., 2016).

2.4 Meteorological Controls

The relationship between *f* and Δ*d* in precipitation is related to different meteorological conditions (Kern et al., 2020; Wang et al., 2016). Figure 7 shows the relationship between *f* and Δ*d* in precipitation on different meteorological conditions at Urumqi Glacier No. 1, including temperature, relative humidity and precipitation amount. At the temperature between 0 and 4 ℃, the slope of Δ*d*-*f* correlation is 0.90, lower than 1 slightly (Fig. 7a). While when the temperature is between 4 and 6 ℃, the slope is 0.92 (Fig. 7b). At the temperature is above 6 ℃, the slope is 0.87 (Fig. 7c). At the relative humidity is less than 70%, the slope is 0.90 which reflects the low correlation between *f* and Δ*d* (Fig. 7d). The correlation between *f* and Δ*d* is lower when the relative humidity is between 70% and 90%, with the slope of 0.79 (Fig. 7e). When the relative humidity is above 90% and close to 100%, the slope is 0.96 higher than 0.90 slightly (Due to the few points in the graph, there may be significant errors of the results) (Fig. 7f). The variation of the slope of the interrelationship between *f* and Δ*d* is increased with the increasing of precipitation (Figs. 7g, 7h, 7i). When the amount of precipitation is lower than 5 mm, the slope is 0.90. When the amount of precipitation is between 5–10 mm, the slope is 1.05 slightly higher than 1. While when the amount of precipitation is above 10 mm, the slope increases to 1.07 higher than 1. In a nutshell, when the temperature is low and the relative humidity is high, the residual fraction of the raindrop is large and the Δ*d* is low even close to 0, and the slope of the Δ*d*-*f* correlation is lower than 1. When the temperature is high and the relative humidity is low, the residual fraction of the raindrop is low and the Δ*d* is high. The researches in Arid area in China have also indicated that the correlation between *f* and Δ*d* is obvious under the conditions of low temperature, high relative humidity and high precipitation. Conversely, the linear relationship is not obvious under the condition of high temperature, low relative humidity and low precipitation (Kern et al., 2020; Wang et al., 2016). Therefore, the influence of different meteorological environments on sub-cloud secondary evaporation of precipitation cannot be ignored.

Figure 8 shows the relationship between Δ*d* and four meteorological parameters in precipitation at Urumqi Glacier No. 1. When the temperature was below 0 ℃, the Δ*d* value was 0, due to the precipitation were mainly snowfall, and the sub-

Table 4 Relationship of evaporation remaining fraction and Δ*d* for each year

Year	Liner regression	Coefficient of determination (R^2)
2008	$\Delta d = 0.93f - 93.04$	0.98
2009	$\Delta d = 0.86f - 86.23$	0.98
2010	$\Delta d = 0.85f - 85.02$	0.99
2011	$\Delta d = 0.88f - 88.51$	0.98

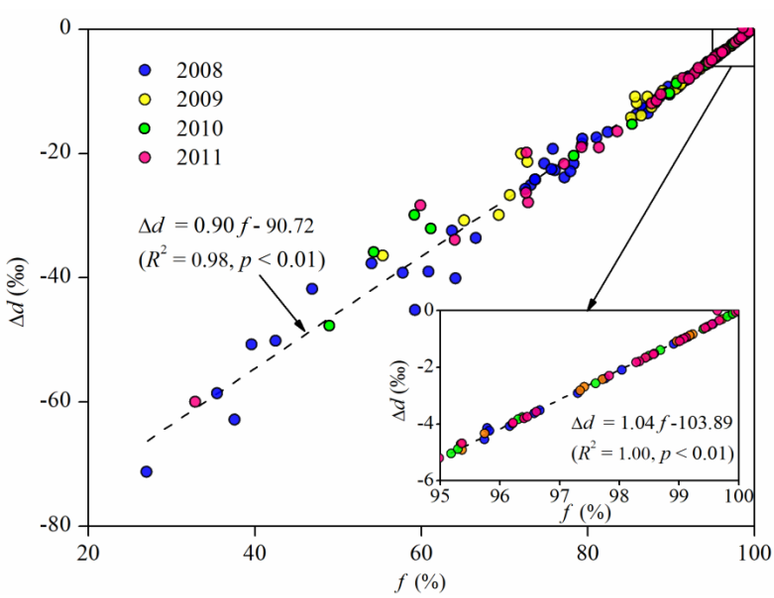

Figure 6. Relationship between *f* and Δ*d* in precipitation events at Urumqi Glacier No. 1 during the observation period.

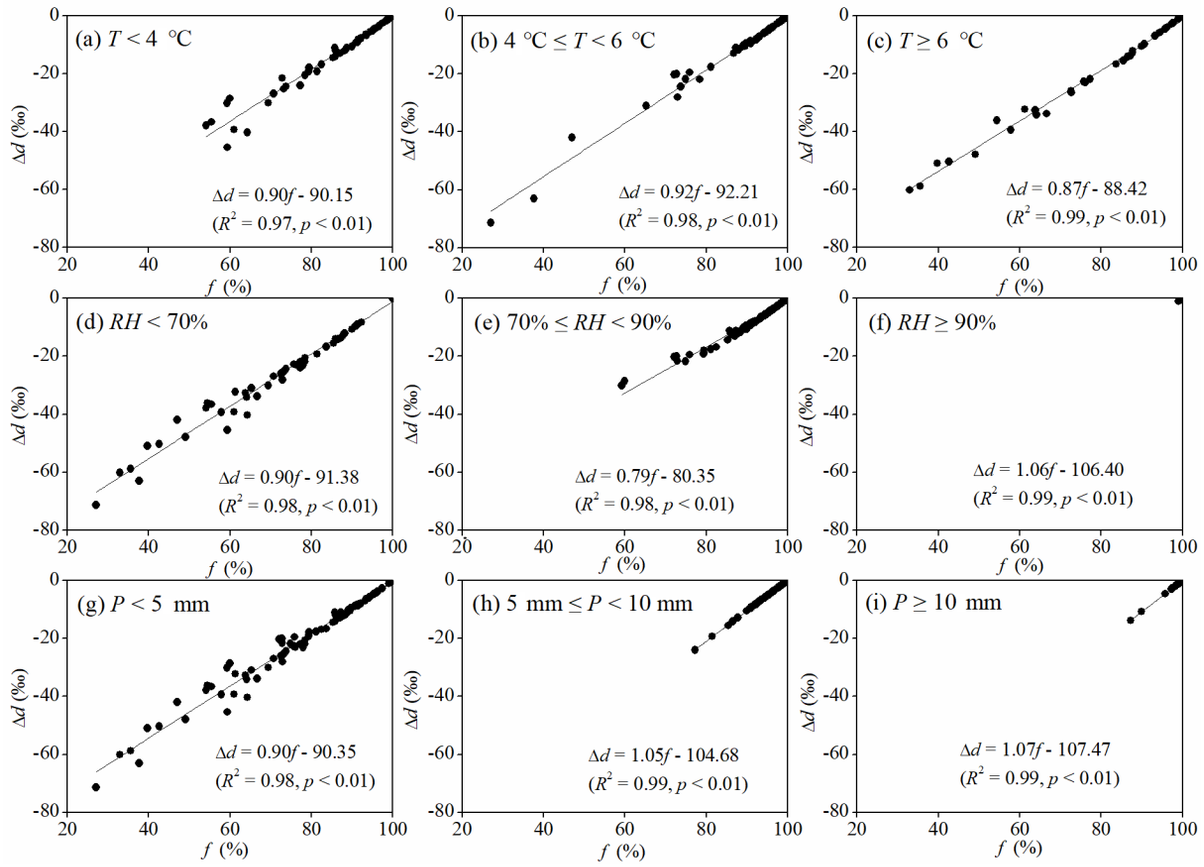

Figure 7. Relationship between f and Δd in daily precipitation at different meteorological conditions at Urumqi Glacier No. 1 from 2008 to 2011. Air temperature (T, (a)–(c)), relative humidity (RH, (d)–(f)), precipitation amount (P, (g)–(i)).

cloud evaporation was usually negligible (Fig. 8a). With the increasing of temperature from 0 °C, the Δd value decreased significantly. As the relative humidity increased, the Δd value inclined to 0. While when the relative humidity ranged from 90% to 100%, the change of Δd value was little (Fig. 8b). When the amount of precipitation was low, the Δd value changed greatly from 0 to -80‰ (Fig. 8c). While with the increasing precipitation amount, the change of Δd value was small and even closed to 0. While with the raindrop diameter increased, the Δd value also ended to be 0 (Fig. 8d). The effect of the four meteorological parameters on Δd is similar to that in Tianshan Mountains, and the effect of relative humidity is more obvious (Wang et al., 2016).

The observation of raindrops diameter is minimal at the glacial area in Tianshan. There are reports of raindrop diameters on the north and south slopes, and the mountainous areas of the Tianshan. The raindrops diameters at Urumqi Glacier No. 1 range from 0.47 to 1.99 mm, with an average value of 1.13 mm, and the mid-value of 1.14 mm. The change of raindrop diameter also has a certain influence on the strength of secondary evaporation (Ma et al., 2020; Wang et al., 2016). Therefore, the f and Δd values in raindrops are recalculated with the constant diameter from 0.4 to 1.9 mm by a step width of 0.1 mm (Fig. 9). The effect of raindrop diameter on f and Δd in precipitation is obvious. When the raindrop diameter is above 1 mm, the f is larger than 90% and the values of Δd are higher than -10‰. When the raindrop diameter is lower than 1 mm, the Δd is lower than -20‰. Therefore, the influence of raindrops diameter on f and Δd cannot be ignored at Urumqi Glacier No. 1. When using the Stewart model, it is not advisable to consider the raindrop diameter as a constant in this study area.

3 CONCLUSION

In this study, the influence of meteorological parameters on sub-cloud secondary evaporation in terms of its isotopic composition is investigated. The variation of d-excess values and the parameters of the δ^2H-$\delta^{18}O$ correlation equation in different meteorological conditions suggest a secondary evaporation effect under the clouds in this area. The slope and intercept of the δ^2H-$\delta^{18}O$ correlation equation and the d-excess values increased with the increasing of precipitation amount. The results suggest that secondary evaporation is significant when the rainfall event is small, while it is not significant for the snow samples. Except for the precipitation samples below 0 °C, the values of d-excess, slope and intercept decreased with the temperature increased, and the influence of secondary evaporation in precipitation enhanced. In addition, as the samples below 0 °C are generally snow samples, the secondary evaporation effect is not apparent. With the relative humidity increase, d-excess value, slope and intercept decrease, which indicated that the secondary evaporation enhanced. The values of f and Δd in raindrops from cloud base to ground are simulated quantitatively using the Stewart model at Urumqi Glacier No. 1 from May

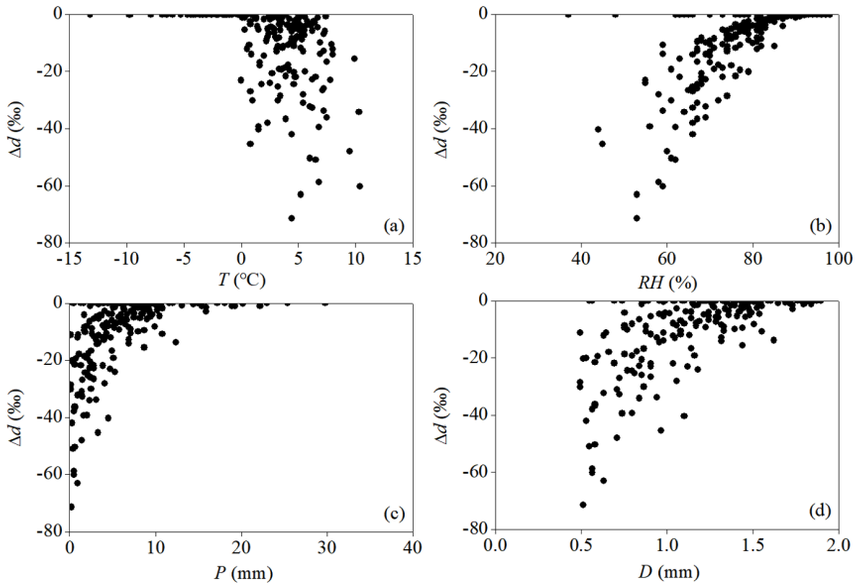

Figure 8. Relationship between Δ*d* and meteorological parameters (*T*, *RH*, *P*, and *D*) in daily precipitation at Urumqi Glacier No. 1.

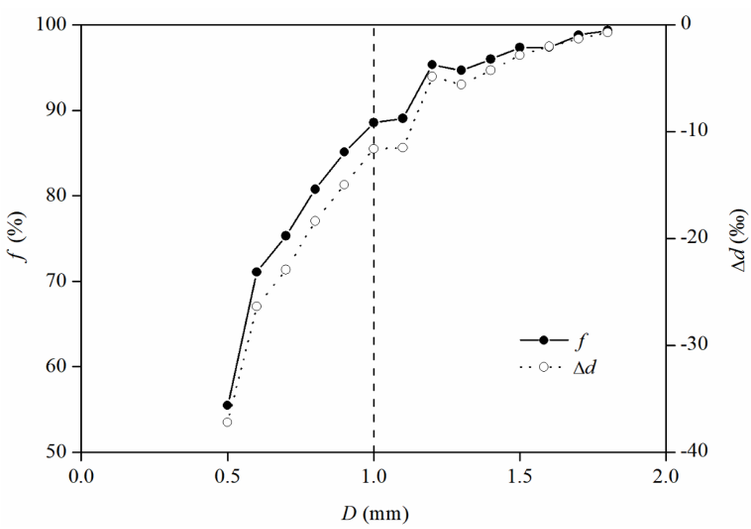

Figure 9. Relationship between raindrop diameter (*D*) and *f* or Δ*d* in precipitation at Urumqi Glacier No. 1.

to September. The results show that the values of *d*-excess decreased from the cloud base to the ground. There is a certain correlation between the *f* and Δ*d* (R^2 = 0.98, $p < 0.01$) in the event-based precipitation of Urumqi Glacier No. 1. For every 1% increase in evaporation, the *d*-excess in the raindrops decreased by 0.90‰ approximately. When the remaining fraction of raindrop mass is above 95%, the regression slope between *f* and Δ*d* is close to 1%/‰, and the liner correlation is good, with the raindrop mass evaporation increases by 1%, *d*-excess in precipitation decreases by approximately 1.04‰. In the high temperature, low relative humidity, small raindrop diameter and amount of precipitation environment, the values of *f* are small and the values of Δ*d* are large. While in the high relative humidity, low temperature, large raindrop diameter and amount of precipitation environment, the *f* values are large and the Δ*d* values are small relatively.

In the alpine and cold regions, especially in the glacierized area, the constant linear relationship of approximately 1‰ between evaporation of raindrop and *d*-excess should not be quoted directly. Not only the influence of meteorological factors on sub-cloud secondary evaporation on precipitation, but also the influence of raindrop diameter should be considered. When using the isotope-evaporation model, due to the change of the value method, the practicability of the parameters should be fully considered and optimized. At Urumqi Glacier No. 1 with limited observation conditions, it is necessary to use the optimized parameter model for quantitative evaluation in precipitation.

ACKNOWLEDGMENTS

We thank the scientific investigation team working at Tianshan Glaciological Station for help ing collect samples. We also gratefully thank the reviewers for their constructive comments. We thank Daxigou Meteorological Station for supplying the meteorological data. We thank Yuman Zhu at Tianshan Glaciological Station for analyzing the samples. This re-

search was funded by The Second Tibetan Plateau Scientific Expedition and Research (No. 2019QZKK0201), the Strategic Priority Research Program of Chinese Academy of Sciences (Class A) (Nos. XDA20060201, XDA20020102), the National Natural Science Foundation of China (Nos. 41761134093, 41471058) and The SKLCS founding (No. SKLCS-ZZ-2020). The final publication is available at Springer via https://doi.org/10.1007/s12583-021-1522-z.

Conflict of Interest

The authors declare that they have no conflict of interest.

REFERENCES CITED

Barnes, S. L., 1968. An Empirical Shortcut to the Calculation of Temperature and Pressure at the Lifted Condensation Level. *Journal of Applied Meteorology*, 7(3): 511. https://doi.org/10.1175/1520-0450(1968)0070511:aesttc>2.0.co;2

Cao, L., Shen J. M., Nie Z. L., 2021. Stable Isotopic Characteristics of Precipitation and Moisture Recycling in Badain Jaran Desert. *Earth Science*, 46(8): 2973-2983 (in Chinese with English Abstract).

Chen, F. L., Zhang, M. J., Wang, S. J., et al., 2015. Relationship between Sub-Cloud Secondary Evaporation and Stable Isotopes in Precipitation of Lanzhou and Surrounding Area. *Quaternary International*, 380/381: 68–74. https://doi.org/10.1016/j.quaint.2014.12.051

Chen, H. Y., Chen, Y. N., Li, D. L., et al., 2020. Effect of Sub-Cloud Evaporation on Precipitation in the Tianshan Mountains (Central Asia) under the Influence of Global Warming. *Hydrological Processes*, 34(26): 5557–5566. https://doi.org/10.1002/hyp.13969

Christner, E., Aemisegger, F., Pfahl, S., et al., 2018. The Climatological Impacts of Continental Surface Evaporation, Rainout, and Subcloud Processes on δD of Water Vapor and Precipitation in Europe. *Journal of Geophysical Research*: *Atmospheres*, 123(8): 4390–4409. https://doi.org/10.1002/2017jd027260

Crawford, J., Hughes, C. E., Lykoudis, S., 2014. Alternative Least Squares Methods for Determining the Meteoric Water Line, Demonstrated Using GNIP Data. *Journal of Hydrology*, 519: 2331–2340. https://doi.org/10.1016/j.jhydrol.2014.10.033

Criss, R., 1999. Principles of Stable Isotope Distribution. Oxford University, New York. https://doi.org/10.1093/oso/9780195117752.001.0001

Dansgaard, W., 1964. Stable Isotopes in Precipitation. *Tellus*, 16(4): 436–468. https://doi.org/10.1111/j.2153-3490.1964.tb00181.x

Ding, Y. J., Zhang, S. Q., Zhao, L., et al., 2019. Global Warming Weakening the Inherent Stability of Glaciers and Permafrost. *Science Bulletin*, 64(4): 245–253. https://doi.org/10.1016/j.scib.2018.12.028

Feng, F., Li, Z. Q., Zhang, M. J., et al., 2013. Deuterium and Oxygen 18 in Precipitation and Atmospheric Moisture in the Upper Urumqi River Basin, Eastern Tianshan Mountains. *Environmental Earth Sciences*, 68(4): 1199–1209. https://doi.org/10.1007/s12665-012-1820-y

Fletcher, J. K., Bretherton, C. S., 2010. Evaluating Boundary Layer-Based Mass Flux Closures Using Cloud-Resolving Model Simulations of Deep Convection. *Journal of the Atmospheric Sciences*, 67(7): 2212–2225. https://doi.org/10.1175/2010jas3328.1

Fontes, J. C., 1980. Environmental Isotopes in Hydrology. Handbook of Environmental Isotope Geochemistry. Elsevier, Amsterdam. 75–140

Froehlich, K., Kralik, M., Papesch, W., et al., 2008. Deuterium Excess in Precipitation of Alpine Regions-Moisture Recycling. *Isotopes in Environmental and Health Studies*, 44(1): 61–70. https://doi.org/10.1080/10256010801887208

Górnicki, K., Winiczenko, R., Kaleta, A., et al., 2017. Evaluation of Models for the Dew Point Temperature Determination. *Technical Sciences*, 3(20): 241–257. https://doi.org/10.31648/ts.5425

Jouzel, J., Merlivat, L., 1984. Deuterium and Oxygen 18 in Precipitation: Modeling of the Isotopic Effects during Snow Formation. *Journal of Geophysical Research*: *Atmospheres*, 89(D7): 11749–11757. https://doi.org/10.1029/jd089id07p11749

Kern, Z., Hatvani, I., Czuppon, G., et al., 2020. Isotopic 'Altitude' and 'Continental' Effects in Modern Precipitation across the Adriatic-Pannonian Region. *Water*, 12(6): 1797. https://doi.org/10.3390/w12061797

Kinzer, G. D., Gunn, R., 1951. The Evaporation, Temperature and Thermal Relaxation-Time of Freely Falling Waterdrops. *Journal of Meteorology*, 8(2): 71 – 83. https://doi.org/10.1175/1520-0469(1951)0080071:tetatr>2.0.co;2

Kong, Y. L., Pang, Z. H., 2016. A Positive Altitude Gradient of Isotopes in the Precipitation over the Tianshan Mountains: Effects of Moisture Recycling and Sub-Cloud Evaporation. *Journal of Hydrology*, 542: 222–230. https://doi.org/10.1016/j.jhydrol.2016.09.007

Kong, Y. L., Pang, Z. H., Froehlich, K., 2013. Quantifying Recycled Moisture Fraction in Precipitation of an Arid Region Using Deuterium Excess. *Tellus B*: *Chemical and Physical Meteorology*, 65(1): 19251. https://doi.org/10.3402/tellusb.v65i0.19251

Li, Y. G., Li, Z. X., Feng, Q., et al., 2018. Environmental Significance of the Stable Isotopes in Precipitation at Different Altitudes in the Tuolai River Basin. *Environmental Science*, 39(6): 2661–2672. https://doi.org/10.13227/j.hjkx.201708087 (in Chinese with English Abstract)

Li, Z. Q., Li, H. L., Chen, Y. N., 2011. Mechanisms and Simulation of Accelerated Shrinkage of Continental Glaciers: A Case Study of Urumqi Glacier No. 1 in Eastern Tianshan, Central Asia. *Journal of Earth Science*, 22(4): 423 – 430. https://doi.org/10.1007/s12583-011-0194-5

Li, Z. X., Feng, Q., Wang, Y. M., et al., 2016a. Effect of Sub-Cloud Evaporation on the $\delta^{18}O$ of Precipitation in Qilian Mountains and Hexi Corridor, China. *Sciences in Cold and Arid Regions*, 8(5): 378–387

Li, Z. X., Feng, Q., Wang, Q. J., et al., 2016b. The Influence from the Shrinking Cryosphere and Strengthening Evopotranspiration on Hydrologic Process in a Cold Basin, Qilian Mountains. *Global and Planetary Change*, 144: 119–128. https://doi.org/10.1016/j.gloplacha.2016.06.017

Li, Z. X., Gui, J., Wang, X. F., et al., 2019. Water Resources in Inland Regions of Central Asia: Evidence from Stable Isotope Tracing. *Journal of Hydrology*, 570: 1–16. https://doi.org/10.1016/j.jhydrol.2019.01.003

Liu, B., Kang, S. C., Sun, J. M., et al., 2014. Low-Molecular-Weight Organic Acids in the Tibetan Plateau: Results from One-Year of Precipitation Samples at the SET Station. *Atmospheric Environment*, 86: 68–73. https://doi.org/10.1016/j.atmosenv.2013.12.028

Liu, J. R., Song, X. F., Yuan, G. F., et al., 2014. Stable Isotopic Compositions of Precipitation in China. *Tellus B*: *Chemical and Physical Meteorology*, 66(1): 22567. https://doi.org/10.3402/tellusb.v66.22567

Liu, Z. F., Tian, L. D., Yao, T. D., et al., 2008. Seasonal Deuterium Excess in Nagqu Precipitation: Influence of Moisture Transport and Recycling in the Middle of Tibetan Plateau. *Environmental Geology*, 55(7): 1501–1506. https://doi.org/10.1007/s00254-007-1100-4

Lis, G., Wassenaar, L. I., Hendry, M. J., 2008. High-Precision Laser

Spectroscopy D/H and $^{18}O/^{16}O$ Measurements of Microliter Natural Water Samples. *Analytical Chemistry*, 80(1): 287–293. https://doi.org/10.1021/ac701716q

Ma, Q., Zhang, M. J., Wang, S. J., et al., 2014. An Investigation of Moisture Sources and Secondary Evaporation in Lanzhou, Northwest China. *Environmental Earth Sciences*, 71(8): 3375–3385. https://doi. org/10.1007/s12665-013-2728-x

Ma, X. G., Jia, W. X., Zhu, G. F., et al., 2020. Quantitative Analysis of the Sub-Cloud Evaporation of Atmospheric Precipitation and Its Controlling Factors Calculated by D-Excess in an Inland River Basin of China. *Water*, 12(10): 2798. https://doi.org/10.3390/w12102798

Meng, Y. C., Liu, G. D., 2010. Effect of Below-Cloud Secondary Evaporation on the Stable Isotopes in Precipitation over the Yangtze River Basin. *Advances in Water Science*, 21(3): 327–334. https://doi.org/10.14042/j. cnki. 32.1309.2010.03.004 (in Chinese with English Abstract)

Merlivat, L., Jouzel, J., 1979. Global Climatic Interpretation of the Deuterium-Oxygen 18 Relationship for Precipitation. *Journal of Geophysical Research*: *Oceans*, 84(C8): 5029–5033. https://doi. org/10.1029/jc084ic08p05029

Pande, K. C., Padia, J. T., Ramesh, R., et al., 2000. Stable Isotope Systematics of Surface Water Bodies in the Himalayan and Trans-Himalayan (Kashmir) Region. *Journal of Earth System Science*, 109(1): 109–115. https://doi.org/10.1007/BF02719154

Pang, Z. H., Kong, Y. L., Froehlich, K., et al., 2011. Processes Affecting Isotopes in Precipitation of an Arid Region. *Tellus B*: *Chemical and Physical Meteorology*, 63(3): 352–359. https://doi.org/10.1111/j.1600-0889.2011.00532.x

Peng, H. D., Mayer, B., Harris, S., et al., 2007. The Influence of Below-Cloud Secondary Effects on the Stable Isotope Composition of Hydrogen and Oxygen in Precipitation at Calgary, Alberta, Canada. *Tellus B*: *Chemical and Physical Meteorology*, 59(4): 698–704. https://doi.org/10.1111/j.1600-0889.2007.00291.x

Peng, T. R., Wang, C. H., Huang, C. C., et al., 2010. Stable Isotopic Characteristic of Taiwan's Precipitation: A Case Study of Western Pacific Monsoon Region. *Earth and Planetary Science Letters*, 289(3/4): 357–366. https://doi.org/10.1016/j.epsl.2009.11.024

Salamalikis, V., Argiriou, A. A., Dotsika, E., 2016. Isotopic Modeling of the Sub-Cloud Evaporation Effect in Precipitation. *Science of the Total Environment*, 544: 1059–1072. https://doi. org/10.1016/j.scitotenv.2015.11.072

Shi, Y. F., Shen, Y. P., Kang, E. S., et al., 2007. Recent and Future Climate Change in Northwest China. *Climatic Change*, 80(3/4): 379–393. https://doi.org/10.1007/s10584-006-9121-7

Song, M. Y., Li, Z. Q., Xia, D. S., et al., 2019. Isotopic Evidence for the Moisture Origin and Influencing Factors at Urumqi Glacier No. 1 in Upstream Urumqi River Basin, Eastern Tianshan Mountains. *Journal of Mountain Science*, 16(8): 1802–1815. https://doi. org/10.1007/s11629-018-5348-9

Stewart, M. K., 1975. Stable Isotope Fractionation Due to Evaporation and Isotopic Exchange of Falling Waterdrops: Applications to Atmospheric Processes and Evaporation of Lakes. *Journal of Geophysical Research*, 80(9): 1133–1146. https://doi.org/10.1029/jc080i009p01133

Wang, P. Y., Li, Z. Q., Huai, B. J., et al., 2015. Spatial Variability of Glacial Changes and Their Effects on Water Resources in the Chinese Tianshan Mountains during the last Five Decades. *Journal of Arid Land*, 7(6): 717–727. https://doi.org/10.1007/s40333-015-0086-0

Wang, P. Y., Li, Z. Q., Jin, S., et al., 2014. Ice Thickness, Volume and Subglacial Topography of Urumqi Glacier No. 1, Tianshan Mountains, Central Asia, by ground Penetrating Radar Survey. *Journal of Earth System Science*, 123(3): 581–591. https://doi.org/10.1007/s12040-014-0421-4

Wang, R., Liu, Z. F., 2020. Stable Isotope Evidence for Recent Global Warming Hiatus. *Journal of Earth Science*, 31(2): 419–424. https://doi.org/10.1007/s12583-019-1239-4

Wang, S. J., Jiao, R., Zhang, M. J., et al., 2021. Changes in Below-Cloud Evaporation Affect Precipitation Isotopes during Five Decades of Warming across China. *Journal of Geophysical Research*: *Atmospheres*, 126(7): e2020JD033075. https://doi.org/10.1029/2020jd033075

Wang, S. J., Zhang, M. J., Crawford, J., et al., 2017. The Effect of Moisture Source and Synoptic Conditions on Precipitation Isotopes in Arid Central Asia. *Journal of Geophysical Research*: *Atmospheres*, 122(5): 2667–2682. https://doi.org/10.1002/2015jd024626

Wang, S. J., Zhang, M. J., Che, Y. J., et al., 2016. Influence of Below-Cloud Evaporation on Deuterium Excess in Precipitation of Arid Central Asia and Its Meteorological Controls. *Journal of Hydrometeorology*, 17(7): 1973–1984. https://doi.org/10.1175/jhm-d-15-0203.1

Wang, S. J., Zhang, M. J., Sun, M. P., et al., 2013. Changes in Precipitation Extremes in Alpine Areas of the Chinese Tianshan Mountains, Central Asia, 1961-2011. *Quaternary International*, 311: 97–107. https://doi.org/10.1016/j.quaint.2013.07.008

Wang, X. Y., Li, Z. Q., Tayier, R., et al., 2015. Characteristics of Atmospheric Precipitation Isotopes and Isotopic Evidence for the Moisture Origin in Yushugou River Basin, Eastern Tianshan Mountains, China. *Quaternary International*, 380/381: 106–115. https://doi.org/10.1016/j.quaint.2014.12.023

Wu, H. W., Zhang, X. P., Li, X. Y., et al., 2015. Seasonal Variations of Deuterium and Oxygen-18 Isotopes and Their Response to Moisture Source for Precipitation Events in the Subtropical Monsoon Region. *Hydrological Processes*, 29(1): 90–102. https://doi. org/10.1002/hyp.10132

Xu, C. H., Li, Z. Q., Li, H. L., et al., 2019. Long-Range Terrestrial Laser Scanning Measurements of Annual and Intra-Annual Mass Balances for Urumqi Glacier No. 1, Eastern Tien Shan, China. *The Cryosphere*, 13(9): 2361–2383. https://doi.org/10.5194/tc-13-2361-2019

Yapp, C. J., 1982. A Model for the Relationships between Precipitation D/H Ratios and Precipitation Intensity. *Journal of Geophysical Research*: *Oceans*, 87(C12): 9614–9620. https://doi. org/10.1029/jc087ic12p09614

Yu, T. T., Gan, Y. Q., Zhou, A. G., et al., 2010. Characteristics of Oxygen and Hydrogen Isotope Distribution of Surface Runoff in the Lhasa River Basin. *Earth Science*, 35(5): 873–878 (in Chinese with English Abstract)

Zhang, X. P., Yao, T. D., Liu, J. M., et al., 2003. Simulations of Stable Isotopic Fractionation in Mixed Cloud in Middle Latitudes-Taking the Precipitation at Urumqi as an Example. *Advances in Atmospheric Sciences*, 20(2): 261–268 (in Chinese with English Abstract)

Zheng, J., Fan, J. L., Zhang, F. C., 2019. Spatiotemporal Trends of Temperature and Precipitation Extremes across Contrasting Climatic Zones of China during 1956–2015. *Theoretical and Applied Climatology*, 138(3/4): 1877 – 1897. https://doi. org/10.1007/s00704-019-02942-5

Zhu, G. F., Li, J. F., Shi, P. J., et al., 2016. Relationship between Sub-Cloud Secondary Evaporation and Stable Isotope in Precipitation in Different Regions of China. *Environmental Earth Sciences*, 75(10): 1–18. https://doi.org/10.1007/s12665-016-5590-9